ISSN 0511-5728
The West Indian Journal of Engineering
Vol.42, No.1, July 2019, pp.39-50

CubeSat Communication Sub-system Design for Coastal Marine Monitoring Applications

Richelle V. Adams [a, Ψ], Deborah Villarroel-Lamb[b], and Fasil Muddeen[c]

[a] Department of Electrical and Computer Engineering, The University of the West Indies, St. Augustine Campus, Trinidad and Tobago, West Indies; E-mail: Richelle.Adams@sta.uwi.edu

[b] Department of Civil Engineering, The University of the West Indies, St. Augustine Campus, Trinidad and Tobago, West Indies: Email: Deborah.Villarroel-Lamb@sta.uwi.edu

[c] Department of Electrical and Computer Engineering, The University of the West Indies, St. Augustine Campus, Trinidad and Tobago, West Indies; Email: Fasil.Muddeen@sta.uwi.edu

[Ψ] *Corresponding Author*

(Received 24 January 2019; Revised 09 April 2019; Accepted 17 June 2019)

Abstract: *In this paper, we present a design for a CubeSat communication subsystem for a store-and-forward remote monitoring application that will transfer data which originates from an underwater Acoustic Doppler Current Profiler (ADCP) at a remote coastal location to a central hub for processing. For this design we determined the bandwidth requirements of the ADCP; performed the LEO constellation design for different orbital altitudes; determined, with the aid of AGI's STK simulation tool, the worst-case bit-rate that can be accommodated during the visible period; explored different frequency bands for transmission with the UHF/VHF and the S-band being selected as like candidates; designed the antenna; selected transceivers for the ground station and CubeSat; and performed link budgets for the different altitudes. Additionally, the paper discusses CubeSat design considerations and other terrestrial and non-terrestrial transmission alternatives to CubeSat.*

Keywords: *CubeSat; nano-satellites; Acoustic Doppler Current Profiler; ADCP; communication design*

1. Introduction

Ocean hydrodynamic data collection is an essential exercise in the long-term planning and development of adaptation strategies for any coastal environment. In Small Island Developing States (SIDS), such as a number of islands in the Caribbean region, the comprehensive data collection to effect these activities is limited by a number of factors. While these factors are varied depending on the country, they include access to technologies and innovations that can facilitate an effective and remote communication of continuous oceanographic parameters such as wave and current attributes.

Regionally, data collection of these parameters may involve the deployment of a wave gauge (for example an Acoustic Doppler Current Profiler (ADCP)) at given locations where the data is retrieved directly from the device. The period of deployment is contingent upon the battery life and the rate of data collection. Other methods for data collection exist for in situ measurements, such as wave buoys or wave staffs (waves only) or remote sensing techniques may be implemented. The method where data are retrieved directly from the device is suitable for short-term deployments, but proves inefficient in long-term data collection. Remote sensing techniques which may be land-based (video imagery), airborne or satellite-borne are more apt in terms of efficient data retrieval. Notwithstanding, in-situ measurements are required for most ocean engineering applications (Chen-Tung and Nihoul, 2009).

Remotely retrieving data from an in situ device can facilitate a near real-time data access, which provides more ready evaluation of observed parameters at a localized area: ready evaluation of hydrodynamic data is especially essential for coastal environments of smaller islands. In addition, wave measurements in shallow or intermediate water, which have localized characteristics, are required for long-term planning. Some challenges for setting up a system where data is retrieved remotely from an in-situ device deployed in the long-term include:

- The determination of whether a shallow water deployment is suitable for long term wave assessment at the given location,
- The determination of the suitability of a bottom-mount or a surface floating wave device at that location,
- The security or the safety of the deployed device, especially in shallower waters,
- The access to a continuous power supply; batteries will need to be changed and inherently involve some period of down-time of the device unless there is some instrumentation redundancy,

- The reduction of marine bio-fouling to bottom-mounted instruments,
- The assessment of any conflict of the deployed system with other users, such as interference with shipping or navigational routes,
- The assessment of any impact from hurricanes/storms which may affect the deployed device, such as covering with sediment or displacement of the instrument, and
- The determination of the most cost-effective and efficient method of data-retrieval.

This paper seeks to specifically address the issue of efficient remote data-retrieval for a regional data collection system targeting the acquisition of the hydrodynamic parameters of waves and currents. The proposed system focuses on the application of CubeSat technology which is considered to be a novel and feasible solution.

While we propose to discuss the CubeSat design process and its many considerations, it is instructive to indicate the alternative technologies that can be used for the ADCP remote-data-removal application. Terrestrial options include: Amateur Radio (Wilson, 2007), General Packet Radio Service (GPRS) (Kong et al., 2005; Zhao et al., 2012a,b), Long Term Evolution (LTE) (He et al., 2016; Julio, 2016; Ratasuk et al., 2013); Satellite options: Iridium (Fossa et al., 1998), Inmarsat (Pedersen et al., 2015; Jun-lin and Chun-sheng, 2011); Non-satellite, non-terrestrial: BalloonSats (Shiroma et al., 2012), Airborne Remote Communication (ARC) Platform (Weinert et al., 2012).

One value proposition for CubeSat technology is its relatively low cost compared to commercial satellite systems (Schaffner, 2002) which makes satellite technology more accessible to academic institutions wishing to conduct satellite system design and perform satellite missions (Schaffner, 2002; Preindl et al., 2009b; Shiroma et al., 2012; Khurshid et al., 2013; Blas, 2009). Additionally, it opens opportunities for developing countries with limited resources to pursue advanced satellite programs of their own. One major cost component of any satellite programme is that of the launch. To significantly reduce this cost, Cal Poly developed a common deployer for picosatellites called the P-POD (Poly Picosatellite Orbital Deployer), which, as a consequence, enforces standard dimensions of the form-factor and functionality for the picosatellites. Restricting their mass, volume and surface area makes the design of CubeSats very challenging (Schaffner, 2002).

CubeSats are deployed in (low-earth-orbit) LEO orbits, so that unlike their (Geostationary Satellites) GEO counterparts which maintain static coverage bas they rotate at the same rate as the earth, their coverage is not constant over a geographic region. Therefore, there is a limited viewing time or contact time between the satellite and the ground station (Kiremitci, 2013; Preindl et al., 2009b). This exacerbates the low data rate problem. However, the lower orbit, the smaller the free-space loss to overcome, and therefore the less the power that would be required for signal transmission.

In Section 2, we present the CubeSat design for the ADCP system. There, we perform the ADCP bandwidth calculations, the LEO constellation design, frequency selection, antenna design, transceiver selection and link budgets. We conclude in Section 3.

2. Design

The satellite system architecture consists of a number of subsystems or modules, i.e., antennas; battery and power system; thermal control; propulsion system; onboard data handling (OBDH); payload module; attitude determination and control system (ADCS); uplink/downlink communication module (Gao et al., 2009); and structure subsystem (Waydo et al., 2002). The focus of this paper would be the design of the communication module.

2.1. ADCP Bandwidth Calculations

The ADCP e used in this assessment was a WorkHorse Sentinel (WHSZ1200 WH Sentinel 1200 kHz SC ADCP) which is specifically designed for short- to medium-term (weeks to months) autonomous deployment from either a temporary or permanent mounting (Teledyne RD Instruments, 2013). This device has the standard housing which allows deployment to water depths of a maximum of 200m. The ADCP may be configured to collect both current speed and direction at various elevations within the water column, as well as, wave height measurements. The sampling rate may be specified, but the recommended rate is typically employed which is 10 minutes between averaged ensembles for the current data collection, and for the wave data a 20 minute burst duration with 60 minutes between the start of bursts using 2,400 samples per burst. The standard battery pack is used and at the recommended sampling rate allows for approximately a six-week deployment. Battery life may be extended for longer term deployments through use of an external battery case which holds two additional battery packs.

As an alternative, a lithium battery pack may be used instead of the standard alkaline battery pack and this should provide about three times the capacity of the standard alkaline battery pack (Teledyne RD Instruments, personal communication). Consideration may be given to use of an external power supply for longer-term deployments, such as a solar power supply. However, if this option is pursued, care must be taken to ensure that the ADCPs specific power requirements are satisfied. The 256MB memory card is adequate for these 6-week deployments, but a larger capacity memory card may be used if required. Data storage and retrieval are critical aspects of the monitoring application.

One common method to facilitate data transmission remotely is through use of an acoustic modem (Teledyne RD Instruments, 2019). This arrangement would require that two modems be installed: one near the ADCP (underwater for bottom deployments) and one at the surface (on a buoy or at some structure onshore). The surface modem receives the data which is transmitted acoustically from the ADCP via the underwater modem unit (Teledyne RD Instruments, 2019). This surface modem can then be connected directly to a computer or be routed through some wireless network such as radio, cellular (3G or 4G) or satellite.

The overall system diagram is shown in Figure 1 and, the data requirements calculated for the ADCP can be found in Table 1. The assumptions include that a comma-separated-values (CSV) file with comma separators will be used to store the information with possible carriage return (CR)/line feed (LF) between burst records. Fixed field widths are also assumed.

From Table 1, the CSV file size increases by 84+38 (39) = 122 (123) bytes= 976 (984) bits per burst. Currently, there is one burst per hour, but it can be configured for up to three to four bursts per hour.

Additionally data currency, data integrity and data repudiability should be considered. In terms of data currency, ideally the data should arrive at the endpoint within 3 to 60 minutes of sampling. In terms of data integrity, ideally the data should arrive without error. The simplest approach to enhance data integrity would be to repeat the transmission of the data three (3) times. In terms of data repudiability, the source of the data should be verified, therefore there should be the use of encryption. The overhead due to the encryption should increase the file size to roughly 1.05 times its original size with a minimum of 128 bytes (Stapko, 2010).

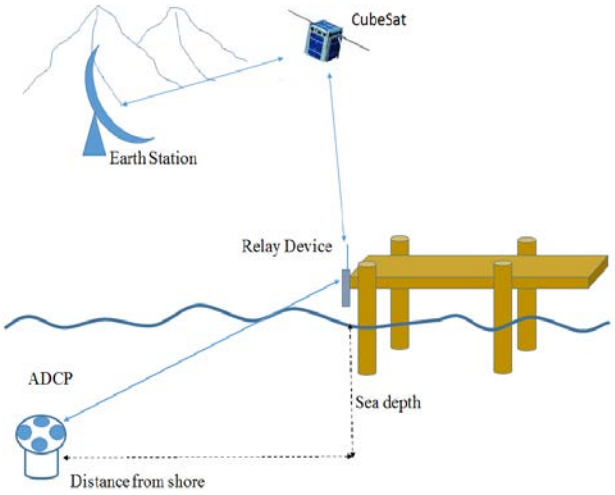

Figure 1. ADCP-CubeSat Communications Diagram

Table 1. ADCP data requirements for a single burst

	Field Size in Characters	Size	Delimiter	Size
Burst #	5	5	Comma	1
Time/Date	14	14	Comma	7
Hs (metres)	3	3	DP, Comma	2
Tp (seconds)	3	3	DP, Comma	2
Dp (degrees)	4	4	DP, Comma	2
Depth (mm)	5.3	8	DP, Comma	2
H1/10 (meters)	3	3	DP, Comma	2
TMean(seconds)	3	3	DP, Comma	2
DMean(degrees)	4	4	DP, Comma	2
#bins	2	2	Comma	1
Subtotal Header		49		23
*#bins Depth level Current Magnitude (m/s)	4	4	DP, Comma	2
*#bins Depth Level Current Direction (degrees)	3	3	Comma (and/or record end)	1 (2)
Subtotal Data (5 bins)		35		15 (16)
Total		84		38 (39)

2.2. LEO Constellation Design

The design goals of the mission is directly influenced by the choice of orbit altitude (Long, 2014; Ravanbakhsh and Franchini, 2013), since altitude determines the free-space path loss, which in turn impacts the choice of other parameters such as antenna gains, transmit power and figure of merit. The choice of altitude also determines the visibility times and the number of passes during a full-revolution of the earth. Other considerations in the choice of orbit altitude include the drag of the earth's atmosphere (at too low an altitude) and the existence of Van Allen belts (at higher altitude). Besides altitude, in the orbital design one may try to determine the number of planes required for the extent of coverage over the specified geographical area, the number of satellites per plane, the inclination of the plane, the inter-plane spacing (Kiremitci, 2013). This is typically determined with the aid of satellite simulation software. Increasing the number of satellites and planes increases coverage but significantly increases the launch cost.

For circular (i.e., equatorial, polar, or inclined) orbit at different altitudes, orbital parameters such as satellite velocity at altitude; orbital period; percentage coverage of the earth's surface covered by satellite; slant range at minimum elevation; propagation time of the signal from the earth station to the satellite; number of full revolutions of the satellite around the earth during revisit time; duration the satellite is visible in same direction (prograde); and duration the satellite is visible in opposite direction (retrograde) were determined using equations from Gagliardi (1984). These values are shown in Table 2.

Using the simulation tool by AGI called Systems Tool Kit (STK) 11 (AGI, 2019), multiple orbits were examined at different altitudes and RAAN for coverage and capacity optimization. The orbital inclination chosen was 25° since the target region is primarily the Caribbean.

In Table 3, we show the worst-case bitrate that can be accommodated during the visible period for four different constellations, namely single-orbit (0°), two-

orbit (0°, 90°), three-orbit (0°, 60°, 120°), and six-orbit (0°, 30°, 60°, 90°, 120°, 150°). These were calculated as:

$$\text{worst-case bit-rate} = \frac{B \times N \times R \times X \times L_{\max}}{3600 V_{\min} \times (1 - D_t)} \quad (1)$$

where

B = No. of bits per burst = 984
N = No. of bursts per hour = 4
R = No. of repetitions for data integrity = 3
X = Factor for data repudability = 1.05
$L_{\max}$ = Maximum lapse time in seconds
$V_{\min}$ = Minimum visibility duration in seconds
D_t = Discount for time synchronization = 10%

2.3. Antenna Design

For a CubeSat system, antennas would be required for telemetry, tracking and command (uplink and downlink),

Table 2. Single orbit parameters at different altitudes

Altitude (km)	***h***	**300**	**400**	**500**	**600**	**700**	**800**	**900**
Satellite velocity (km/s)	v_s	7.726	7.668	7.613	7.558	7.504	7.452	7.401
Orbital period (s)	*ts*	5431	5553	5676	5801	5926	6052	6179
Coverage area (km^2)	*A*	3770042	5655500	7642231	9687084	11762844	13851370	15940111
Percentage coverage	A_p	0.738	1.106	1.495	1.895	2.301	2.710	3.118
Slant range (km)	*d*	1160.383	1439.827	1695.081	1932.245	2155.265	2366.867	2569.022
Propagation time (s)	*tp*	0.00387	0.00480	0.00565	0.00645	0.00719	0.00790	0.00857
Visibility time (prograde) (s)	tv_p	298	374	444	511	576	639	700
Visibility time (retrograde) (s)	tv_r	296	372	442	509	573	636	697
Revolutions	*K*1	15.9	15.6	15.2	14.9	14.6	14.3	14.0
Altitude (km)	**h**	**1000**	**1100**	**1200**	**1300**	**1400**	**1500**	
Satellite velocity (km/s)	v_s	7.350	7.301	7.253	7.205	7.159	7.113	
Orbital period (s)	*ts*	6307	6436	6565	6696	6827	6959	
Coverage area (km^2)	*A*	18020153	20085056	22130121	24151907	26147897	28116275	
Percentage coverage	A_p	3.525	3.929	4.329	4.725	5.115	5.500	
Slant range (km)	*d*	2763.211	2950.577	3132.026	3308.287	3479.957	3647.534	
Propagation time (s)	*tp*	0.00922	0.00984	0.0104	0.0110	0.0116	0.0122	
Visibility time (prograde) (s)	tv_p	760	819	878	936	993	1051	
Visibility time (retrograde) (s)	tv_r	757	816	874	932	990	1047	
Revolutions	*K*1	13.7	13.4	13.2	12.9	12.7	12.4	

Table 3. Worst-case bit-rates for different constellations

Altitude (km)	**Single Orbit**			**Two Orbit**		
	Minimum View Time (s)	**Maximum Lapse (s)**	**Worst-Case Bit-Rate (bps)**	**Minimum View Time (s)**	**Maximum Lapse (s)**	**Worst-Case Bit-Rate (bps)**
300	134	34720	1115.59	134	18597	597.54
400	240	41071	736.81	163	18885	498.84
500	470	36045	330.20	470	13355	122.34
600	247	30837	537.53	247	13562	236.40
700	201	31376	672.10	201	7738	165.75
800	201	31376	672.10	201	7738	165.75
900	501	26216	225.30	79	7819	426.14
1000	400	26681	287.19	250	6222	107.16
1100	238	20562	371.98	238	6135	110.99
1200	509	20849	176.36	230	5920	110.82
1300	322	21178	283.18	205	6093	127.97
1400	478	14394	129.65	392	6130	67.33
1500	229	7240	136.12	227	4761	90.30
Altitude (km)	**Three Orbit**			**Six Orbit**		
	Minimum View Time (s)	**Maximum Lapse (s)**	**Worst-Case Bit-Rate (bps)**	**Minimum View Time (s)**	**Maximum Lapse (s)**	**Worst-Case Bit-Rate (bps)**
300	134	13202	424.19	134	7858	252.49
400	144	7745	231.57	144	5178	154.82
500	145	7751	230.15	145	4948	146.92
600	247	7831	136.51	169	5006	127.54
700	179	5658	136.09	179	4744	114.11
800	179	5658	136.09	179	4744	114.11
900	344	5714	71.52	79	4712	256.81
1000	256	5715	96.12	250	4723	81.34
1100	194	5029	111.61	194	4446	98.67
1200	55	4862	380.61	55	4334	339.28
1300	297	4976	72.14	205	4408	92.58
1400	67	4978	319.90	67	4054	260.52
1500	226	4121	78.51	226	3562	67.86

and the transmission of payload data. Antenna design challenges are also outlined in Gao et al. (2009). These included the constraints of size and low mass; low cost; thermal and radiation resilience; material selection to combat atomic oxygen; and effects of vacuum and micro-gravity. Additionally, one must consider mutual coupling among multiple antennas, interference and electromagnetic scattering due to the satellite structure. In Rodrıguez-Osorio and Ramırez (2012)outlined antenna specifications imposed by the platform (e.g., size, modularity, deployment, attitude constraints, compactness), those imposed by communications (e.g., frequency, bandwidth, gain) and those imposed by the mission (e.g., exploration margin, space environment, cost). Additionally, CubeSats may be outfitted with GPS/GNSS and inter-satellite cross links (with the requisite antennas) (Gao et al., 2009).

Different types of antennas have been designed, deployed and/or assessed for CubeSat systems. These include dipole (Muri et al., 2010; Waydo et al., 2002), monopole (Leao et al., 2013; Blas, 2009.; Murtaza, 2011), helix (Gao et al., 2009; Costantine et al., 2016; Leao et al., 2013; Muri et al., 2010; Murtaza, 2011), patch (Gao et al., 2009; Costantine et al., 2016; Muri et al., 2010; Rodr´ıguez-Osorio and Ram´ırez, 2012; Waydo et al., 2002; Akagi et al., 2008), log-periodic crossed dipole antenna array (Costantine et al., 2016), conical log-spiral antenna (Costantine et al., 2016), three-dimensional antenna (Pittella et al., 2013), turnstile (Addaim et al., 2007), planar antenna array as a phased array (Rodrıguez-Osorio and Ramırez, 2012). The dish reflector, Yagi-Uda and Log-periodic antenna were also discussed by Muri et al. (2010) but were found to be unsuitable options in terms of size and complexity for the satellite itself. However, they can be considered for the ground station equipment as in Preindl et al. (2009b).

Some CubeSat mission failures have been attributed to communication problems and more specifically faulty antenna design (Pittella et al., 2013). However, there are tradeoffs to consider when making antenna design choices. For example, Muri et al. (2010) highlighted the issue of antenna gain versus transmit power, and the power savings that can accrue from a directional antenna. However, directional antennas would need more complex attitude control. Another design consideration proceeding from the mission objectives would be the data-rates to be supported. High data rates would be supported by high antenna gain. This in turn will require sophisticated pointing and tracking systems (Gao et al., 2009).

The following is the design for candidate antennas for the CubeSat, namely monopole, dipole, patch and helical. The parabolic antenna design for the ground station is also presented. The design equations for the dipole, helical, patch and parabolic antennas were obtained from Balanis (2005).

2.3.1. Dipole and Monopole Antennas

Table 4 shows the design parameters for the small dipole, half-wavelength dipole and the quarter-wavelength monopole antennas.

Table 4. Dipole antenna design parameters

	Infinitesimal Dipole $\left(l \ll \frac{\lambda}{50}\right)$	Small Dipole $\left(\frac{\lambda}{50} \ll l \ll \frac{\lambda}{10}\right)$	Half-Wavelength Dipole $\left(l = \frac{\lambda}{2}\right)$	Quarter-Wavelength Monopole $\left(l = \frac{\lambda}{4}\right)$
Directivity, D_0	$\frac{3}{2} = 1.761$ dB	$\frac{3}{2} = 1.761$ dB	1.643 = 2.156 dB	3.286 = 5.167 dB
Input Resistance, R_{in}	$80\pi^2\left(\frac{l}{\lambda}\right)^2\ \Omega$	$20\pi^2\left(\frac{l}{\lambda}\right)^2\ \Omega$	73Ω	36.5Ω

2.3.2. Helical Antenna with Ground Plane

Consider a helix of N turns and having a diameter D with spacing between turns of S. The circumference of the helix is $C = \pi D$ and the pitch angle, α is given as:

$$\alpha = \tan^{-1}\left(\frac{S}{\pi D}\right) \quad (2)$$

$$= \tan^{-1}\left(\frac{S}{C}\right) \quad (3)$$

The total length of the antenna is $L = NS$ and the total length of the wire:

$$L_n = N\sqrt{S^2 + C^2} \quad (4)$$

When the helical antenna is operated in axial (end-fire) mode, there is a major lobe of maximum gain along the axis of the helix. For circular polarization the following conditions should hold:

- $\frac{3}{4}\lambda_0 < C < \frac{4}{3}\lambda_0$ with $C \approx \lambda_0$ for near optimum performance where λ_0 is the free-space wavelength of transmission;
- $S \approx \frac{\lambda_0}{4}$;
- $12^\circ < \alpha < 14^\circ$;
- Diameter of ground plane should $\geq \frac{\lambda_0}{2}$
- $N > 3$

The half-power beamwidth (HPBW) (degrees) $\approx \frac{52\lambda_0^{\frac{3}{2}}}{C\sqrt{NS}}$. The directivity, $D_0 \approx 15N\frac{C^2 S}{\lambda_0^3}$. The input impedance (purely resistive), $R \approx 140\left(\frac{C}{\lambda_0}\right)$, therefore a special feed design is required to reduce the input impedance to match a 50Ω transmission line such as a coaxial cable.

2.3.3. Rectangular Patch (Microstrip) Antenna

Balanis (2005) outlined the following steps in the design of the patch antenna:

(1) Specify the dielectric constant, ϵ_r, of the substrate which separates the strip or patch from the ground plane. Specify the resonant frequency, f_r and the height above the ground plane h where $0.003\lambda_0 \leq h \leq 0.05\lambda_0$ and λ_0 is the free-space wavelength of transmission.

Note: $f_r = \frac{v_0}{\lambda_0}$ where v_0 is the free-space velocity of light. Also, the dielectric constant is usually in the range $2.2 \leq \epsilon_r \leq 12$, preferably at the lower end of the range (together with a large h) for better efficiency and larger bandwidth.

(2) Determine the width W and length L

$$W = \frac{v_0}{2f_r}\sqrt{\frac{2}{\epsilon_r+1}} \quad (5)$$

(3) Determine the effective dielectric constant of the microstrip antenna ($\frac{W}{h} > 1$)

$$\epsilon_{reff} = \frac{\epsilon_r+1}{2} + \frac{\epsilon_r+1}{2}\left[1+12\frac{h}{W}\right]^{-\frac{1}{2}} \quad (6)$$

(4) Determine the extension of the length ΔL

$$\frac{\Delta L}{h} = 0.412\left(\frac{\epsilon_{reff}+0.3}{\epsilon_{reff}-0.258}\right)\left(\frac{\frac{W}{h}+0.264}{\frac{W}{h}+0.8}\right) \quad (7)$$

(5) The actual length of the patch:

$$L = \frac{v_0}{2f_r\sqrt{\epsilon_{reff}}} - 2\Delta L \quad (8)$$

Asymptotically, the directivity ($k_0h << 1$):

$$D_0 = \begin{cases} 3.3\ (= 5.2\ \text{dB}) & W \ll \lambda_0 \\ 4\left(\frac{W}{\lambda_0}\right) & W \gg \lambda_0 \end{cases} \quad (9)$$

$$D_2 = \begin{cases} 6.6\ (= 8.2\ \text{dB}) & W \ll \lambda_0 \\ 8\left(\frac{W}{\lambda_0}\right) & W \gg \lambda_0 \end{cases} \quad (10)$$

2.3.4. Parabolic Antenna

For the gateway (or earth station), the parabolic antenna is a likely prospect. Its directivity, D_0, in terms of its dimensions is as follows:

$$D_0 = \left(\frac{\pi d}{\lambda}\right)^2 \quad (11)$$

Dimensions for the patch antenna for different operating frequencies and dielectric constants were calculated and are shown in Table 5. Similarly, for the helical antenna, dimensions and directivity values are calculated for different frequencies and these are shown in Table 6.

2.4. Communications Sub-system

The communication sub-system is very critical to the CubeSat in realizing its mission which is the transfer of data (observed or other type) to earth. The implementation of the communication sub-system was found to be a major challenge for CubeSats (Popescu et al., 2016).

The communication sub-system consists mainly of a radio transceiver, antenna and possibly a diplexer (Leao et al., 2013) if a single antenna would be transmitting/

Table 5. Patch antenna design for different frequencies and dielectric constants

f (MHz)	er = 2		er = 4		er = 5		er = 12		er = 20	
	W (cm)	L (cm)	W (cm)	L (cm)	W (cm)	L (cm)	W (cm)	L (cm)	W (cm)	L (cm)
145	84.41	72.81	65.38	51.62	59.68	46.20	40.55	29.88	31.90	23.2
440	27.82	23.99	21.55	17.01	19.67	15.22	13.36	9.85	10.51	7.6
2200	5.56	4.80	4.31	3.40	3.93	3.04	2.67	1.97	2.10	1.5
2400	5.10	4.40	3.95	3.12	3.61	2.79	2.45	1.81	1.93	1.4
8175	1.50	1.29	1.16	0.92	1.06	0.82	0.72	0.53	0.57	0.4
8400	1.46	1.26	1.13	0.89	1.03	0.80	0.70	0.52	0.55	0.4

Table 6. Helical antenna design for different frequencies and number of turns, $C = \lambda, S = \frac{\lambda}{4}$

f (MHz)	N = 3				N = 5				N = 8			
	Do (dB)	L (cm)	Ln (cm)	D (cm)	Do (dB)	L (cm)	Ln (cm)	D (cm)	Do (dB)	L (cm)	Ln (cm)	D (cm)
145	10.51	155.07	639.35	65.81	12.73	258.44	1065.58	65.81	14.77	413.51	1704.93	65.81
440	10.51	51.10	210.69	21.69	12.73	85.17	351.16	21.69	14.77	136.27	561.85	21.69
2200	10.51	10.22	42.14	4.34	12.73	17.03	70.23	4.34	14.77	27.25	112.37	4.34
2400	10.51	9.37	38.63	3.98	12.73	15.61	64.38	3.98	14.77	24.98	103.01	3.98
8175	10.51	2.75	11.34	1.17	12.73	4.58	18.90	1.17	14.77	7.33	30.24	1.17
8400	10.51	2.68	11.04	1.14	12.73	4.46	18.39	1.14	14.77	7.14	29.43	1.14
f (MHz)	**N = 10**				**N = 12**				**N = 15**			
	Do (dB)	**L (cm)**	**Ln (cm)**	**D (cm)**	**Do (dB)**	**L (cm)**	**Ln (cm)**	**D (cm)**	**Do (dB)**	**L (cm)**	**Ln (cm)**	**D (cm)**
145	15.74	516.88	2131.17	65.81	16.53	620.26	2557.40	65.81	17.50	775.33	3196.75	65.81
440	15.74	170.34	702.32	21.69	16.53	204.40	842.78	21.69	17.50	255.50	1053.47	21.69
2200	15.74	34.07	140.46	4.34	16.53	40.88	168.56	4.34	17.50	51.10	210.69	4.34
2400	15.74	31.23	128.76	3.98	16.53	37.47	154.51	3.98	17.50	46.84	193.14	3.98
8175	15.74	9.17	37.80	1.17	16.53	11.00	45.36	1.17	17.50	13.75	56.70	1.17
8400	15.74	8.92	36.79	1.14	16.53	10.71	44.15	1.14	17.50	13.38	55.18	1.14

receiving both payload data and telemetry and command data. Systems operating in the UHF (420-450 Mhz)/VHF (120-150 MHz)/ amateur bands typically use Frequency Shift Keying modulation scheme and the AX.25 packet protocol to support data transmission which can support bit rates of 12000 bps and 9600 bps (Leao et al., 2013; Selva and Krejci, 2012; Preindl et al., 2009b; Addaim et al., 2007) (the amateur service more specifically referred to as APRS). Additionally, Gaussian Minimum Shift Keying (GMSK) modulation can be used for Telemetry and Telecommand data (Addaim et al., 2007). According to Palo (2015), some systems use quadrature phase shift keying that can provide bitrates of three Mbps coupled with forward error correction and there are now ten Mbps systems.

The choice of communication system used in the CubeSat must be compatible with ground station equipment (Palo, 2015), in terms of frequency bands of operation, modulation and coding scheme and protocol. Because of the power limitations of CubeSats, for meeting the link budget for successful connection, the gain required at the receiving ground station may exceed what can be practically realized. The communication system is typically realized with commercial off-the shelf transceivers with modifications (Waydo et al., 2002).

A major activity in the design of the communication system is performing the link budget. The purpose of the link budget is to ensure that the signal power that reaches the receiver is sufficiently greater than the minimum required receive power (receiver sensitivity) with reasonable margin to ensure the system performs according to BitError Rate (BER) quality and availability targets. Factors considered as part of the link budget include: Effective Isotropic Radiated Power (EIRP) (determined by the transmit power, transmit antenna gain, transmit feeder losses); losses incurred by the link which include atmospheric loss, polarization loss, rain loss, antenna misalignment loss; and free-space path loss among others. The free-space path loss is dependent on the frequency of transmission and the distance between the satellite and ground station. This distance, for LEO orbit varies in a fly-pass from the largest distancewhen the satellite is just above the horizon with a minimum elevation of 10 degrees (Addaim et al., 2007), to the shortest distance when the satellite is directly overhead, i.e. at the altitude of the orbit (Ichikawa, 2006). The worst-case is used in the link budget (Addaim et al., 2007).

However, Popescu et al. (2016) suggested that the CubeSat transmitter can be dynamically adjusted to maintain a constant SNR although the path loss is varying. Other factors in the link budget pertain to the receiver system. The choice of modulation and coding scheme is driven by the BitError-Rate objective and the factor by which the minimum required signal power must exceed the noise floor (where the noise floor is a factor of the system bandwidth, system temperature and the system noise figure).

Typically, for the receiving side of satellite systems the figure of merit, G/T, is used. It is the ratio of receive antenna gain to the system noise temperature. To make a feasible link budget there will be tradeoffs among the factors just described. For example increasing the EIRP (within regulatory limits) may decrease the G/T required, or keeping the same G/T may improve the data rate (Jun-lin and Chun-sheng 2011). For satellite systems, both uplink and downlink budgets should be carried out. These are outlined in sub-section 2.6.

2.5. Transceivers

The Nano avionics UHF transceiver which supports AX.25 protocol, provides substantial system margin (not taking into account antenna gains), i.e., the difference between the transmit power and receiver sensitivity (33-(-120)=153 dB) is much larger than the other radios. However, it operates in half-duplex mode in UHF (430-440 MHz). The implications of this are two-fold. Firstly, there would have to be strict time synchronization among the CubeSat, the remote station and the ground station to prevent interference when the CubeSat transmits on the same frequency. Secondly, the satellite's visibility time would have to be shared between signal transmission and reception, which means a reduced time for the remote station to transmit its data to the satellite.

The ISIS TRXVU VHF/UHF transceiver has a receiver sensitivity of only -104 dBm. So that for the uplink, the terrestrial transmitter (remote terminal or gateway) should have a higher EIRP, which can be achieved by having a higher transmit power and a moderate gain antenna, or lower transmit power but a much higher gain antenna. For the first case, the power requirements of the earth station would be significant, for the latter case, the narrower radiation beamwidth would require a satellite tracking system. This option was chosen. The selected uplink centre-frequency was 146 MHz, and the downlink was 436 MHz.

To complete the VHF uplink and UHF downlink, the Kenwood TM-D710GA 144/440 dual band transceiver would be selected for the remote terminal and gateway. It provides three output power levels: HI at 50 W; MID at 10 W; and LO at 5 W. Its receiver sensitivity is -16 dBμV.

For the S-band solution, the HiSPICO transmitter and receiver would be used for the downlink. The transmitter (which would be located in the CubeSat) is 100g; the modulation scheme is DQPSK; the RF output power 27 dBm (adjustable in the range 16 dBm to 27 dBm); the data rate is 1.06 Mbps; and the frequency band is 2200-2300 MHz in steps of 100 kHz. The receiver (which would be located at the ground station) has receiver sensitivity of -100 dBm at BER of 10^{-5}. For the S-band uplink, a separate receiver module would be required in the CubeSat, such as the SpaceQuest RX-2000 with corresponding TX-2400 at the ground station. Unfortunately, the dimensions of the RX-2000 will push

the dimensions of the CubeSat to at least 2U instead of 1U.

2.6. Link Budgets

To determine the carrier-to-noise-density ratio, $\frac{C}{N_0}$(dB), at the receiving end of a link, the general formula is as follows:

$$\frac{C}{N_0} = P_t + G_t - L_{tx} - L_{fs} - L_{rain} - L_o - L_{pol} - L_{am} - L_{rx} + \frac{G}{T} + 10\log_{10}(k) \quad (12)$$

where P_t is the transmit power (dB); G_t is the gain of the transmit antenna (dBi); L_{tx} is the transmit feeder loss; L_{fs} is the free-space path loss; L_{rain} is the rain loss; L_o is the atmospheric loss; L_{pol} is the polarization loss; L_{am} is the antenna misalignment loss; L_{rx} is the receive feeder loss; G/T is the figure of merit of the receiver system; and k is the Boltzmann constant (i.e., $1.38 \times 10^{-23} J^{\circ}K^{-1}$). All losses are specified in decibels (i.e., dB).

The free-space path loss is determined as follows:

$$L_{fs} = 32.4 + 20\log10(f)(\text{MHz}) + 20\log10(d)(\text{km}) \quad (13)$$

where f is the frequency of transmission and d is the range of transmission.

If the figure of merit is not explicitly stated for the receiver system, that parameter can be replaced by

$$\frac{G}{T} = G_r - 10\log_{10}(T_{sys}) \quad (14)$$

where G_r is the receive antenna gain and T_{sys} is the system noise temperature calculated as:

$$T_{sys} = T_b + (F - 1)\, T_{ambient} \quad (15)$$

where T_b is the background noise temperature due to galactic and sky noise; F is the noise factor of the system; and $T_{ambient}$ is the ambient temperature usually assumed to be 290 $^{\circ}K$.

The noise power density at the receiver (denoted as N_o) is simply:

$$N_0 = kT_{sys} \quad (16)$$

The actual noise power (i.e., N) at the receiver is

$$N = N_0 \times BW \quad (17)$$

where BW is the bandwidth of the receiver system. Therefore the carrier-to-noise ratio, $\frac{C}{N}$ will be:

$$\frac{C}{N} = \frac{C}{N_0} - 10\log_{10}(BW) \quad (18)$$

Additionally, the energy-per-bit-to-noise-density ratio, $\frac{E_b}{N_0}$, will be;

$$\frac{E_b}{N_0} = \frac{C}{N_0} - 10\log_{10}(R_b) \quad (19)$$

where R_b is the data rate of the source in bits/second.

Depending on the transceiver specifications, the receiver sensitivity, $P_{\min}$, would be provided. In which case, the received power, P_r, (after taking into account the transmitted power, all gains and losses) should exceed the receiver sensitivity by a sufficient margin, FM. The link budget equation then becomes:

$$P_r = P_t + G_t - L_{tx} - L_{fs} - L_{rain} - L_o - L_{pol} - L_{am} - L_{rx} + G_r \quad (20)$$

and

$$P_r - P_{min} > FM \quad (21)$$

The link design is constrained by the requirements of the CubeSat. Therefore, the approach taken in performing the link budget was to set the FM to 5 dB and then determine the antenna gains of the CubeSat, remote terminal and gateway that would be required to meet the budget.

The receiver sensitivity may be expressed in terms of dBμV instead of dBm. Let P denote power in watts dissipated by a resistor, R when a voltage of V volts is across it. For the case of the antenna system we assume that it is matched to $R = 50\Omega$.

$$P = \frac{V^2}{R}$$

$$10\log_{10}P = 10\log_{10}\left(\frac{V^2}{R}\right)$$

$$10\log_{10}P = 20\log_{10}V - 10\log_{10}R$$

$$10\log_{10}\left(\frac{P \times 10^{-3}}{10^{-3}}\right) = 20\log_{10}\left(\frac{V \times 10^{-6}}{10^{-6}}\right) - 10\log_{10}50$$

$$P(\text{dBm}) - 30 = V(\text{dB}\mu\text{V}) - 120 - 17$$

$$P(\text{dBm}) = V(\text{dB}\mu\text{V}) - 107 \quad (22)$$

Some manufacturers provide the noise figure, NF (in dB), of the receiver and not the receiver sensitivity. To obtain an estimate of the receiver sensitivity, knowledge of the modulation scheme and bit-rate is required and the following procedure can be applied:

$$P_{\min}(\text{dB}) = SNR_{\min} + N$$

$$P_{\min}(\text{dB}) = \left(\frac{E_b}{N_0}\right)_{\min} + 10\log_{10}\left(\frac{R_b}{BW}\right) + 10\log_{10}(kT_{sys}BW)$$

$$P_{\min}(\text{dB}) = \left(\frac{E_b}{N_0}\right)_{\min} + 10\log_{10}(R_b) + 10\log_{10}(kT_{sys})$$

$$P_{\min}(\text{dB}) = \left(\frac{E_b}{N_0}\right)_{\min} + 10\log_{10}(R_b) + 10\log_{10}\left(kT_{ambient}\left(10^{\frac{NF}{10}} - 1\right)\right)$$

$$P_{min}(\text{dBm}) = P_{\min}(\text{dB}) + 30 \quad (23)$$

where $SNR_{\min}$ is the minimum acceptable signal-to-noise ratio for the modulation scheme at a given bit-error-rate (BER). For example, the SWIFT-SLX S-Band transceiver, NF=0.75 dB, R_b uplink is 5Mbps. Using BPSK, $\left(\frac{E_b}{N_0}\right)_{min}$ =9.59 dB at BER=10^{-5}, $P_{\min}$(dBm) was calculated to be -104.6 dBm.

For operating frequencies in the GHz region, L_{rain} can be estimated using the International Telecommunications Union recommendation ITU-R P.838-3 (ITU, 2005).

$$L_{rain} = k_r R_{\beta,z}^{\alpha_r} D_{rain} \quad (24)$$

where R is the peak rainfall (in mm/h) at β percentage of time in ITU-Zone Z. For example for the Caribbean (in Region N) the peak rainfall is 95 mm/h 0.01% of the time, and D_{rain} is the portion (in km) of the communication link beneath cloud level calculated at the minimum elevation. We assumed minimum elevation to 10°. Storm clouds can be as high as 15 km.

$$D_{rain} = \left[\left(R_E \sin 10^{\circ}\right)^2 + 2R_E(15) + 15^2\right]^{1/2} - R_E \sin 10^{\circ} = 83.35 \text{ km} \quad (25)$$

The coefficients k_r and α_r are frequency-dependent coefficients. For 2.5GHz with vertical polarization, k_r = 0.0001464 and α_r = 1.0085, so that L_{rain} = 1.20dB.

The minimum and maximum free space path loss, and the Doppler shift could be calculated at different frequencies and altitude. From the antenna gain, one can determine how much gain the CubeSat antenna would have to provide compared to that of the remote node (in the case of the uplink) and the gateway (in the case of the downlink). Consider for example, the UHF/VHF uplink link budget for an altitude of 400 km. The combined antenna gain is 9.0 dB. Therefore, the CubeSat antenna could have 0 dBi gain and the remote station's antenna should provide a 9.0 dB gain. In another possible configuration, the CubeSat antenna could have 3 dBi gain, which then means that the remote station's antenna should provide a 6.0 dB gain. Figure 2 depicts these required total antenna gains for the S-band and VHF/UHFband as a function of satellite altitude.

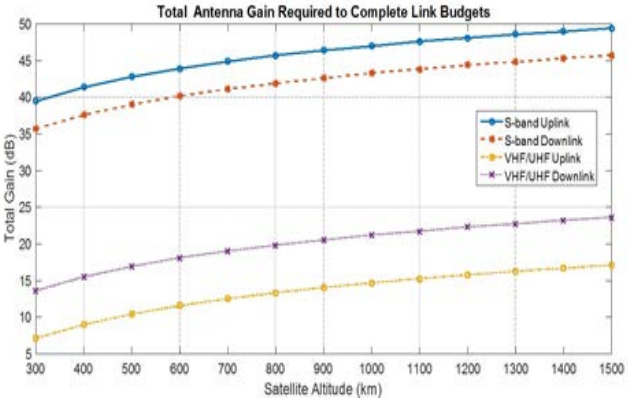

Figure 2. Total antenna gains required to complete link budgets

In Figures 3, 4 and 5, ground station dish diameters are calculated for different satellite altitudes, for when the CubeSat employs a helical antenna of varying turns in the S-band, and when it employs dipole antennas in the VHF/UHF band, respectively.

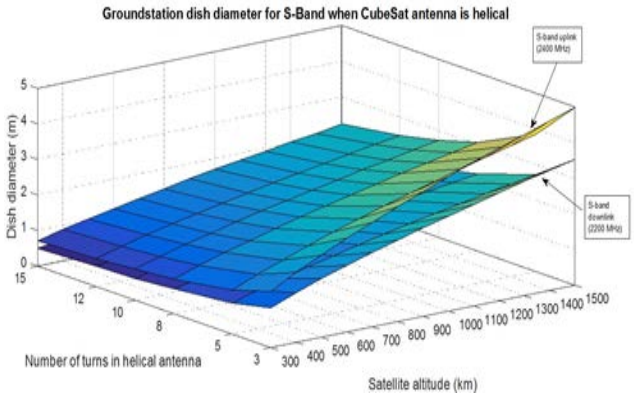

Figure 3. Ground station dish diameters at S-band when CubeSat antenna is helical

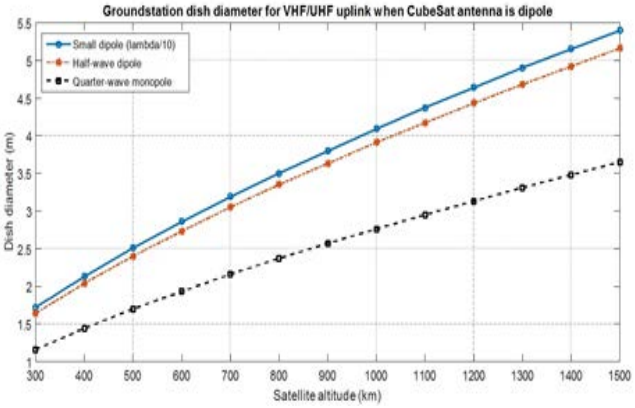

Figure 4. Ground station dish diameters at VHF/UHF uplink when CubeSat antenna is dipole

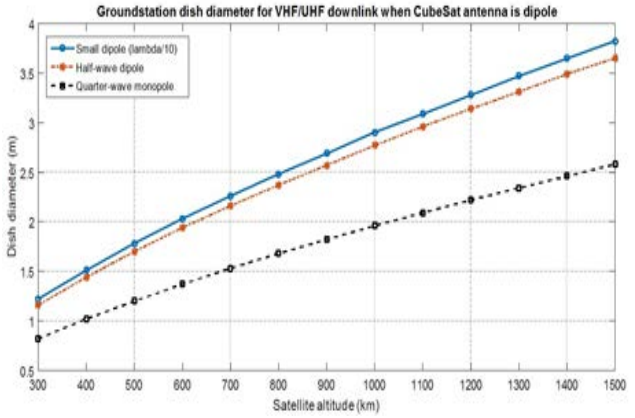

Figure 5. Ground station dish diameters at VHF/UHF downlink when CubeSat antenna is dipole

2.7. Other Design Considerations

Because of the limited space and cost of CubeSats, complex attitude control would be avoided. The attitude control typically adopted would be a passive alignment to the local magnetic field (Leao et al., 2013; Blas, 2009; Addaim et al., 2007) using permanent magnets (Gao et al., 2009).

As a result, the orientation of satellite with respect to the earth cannot be determined beforehand. This then constrains the choice of antenna to an omnidirectional type (Addaim et al., 2007; Leao et al., 2013). Omnidirectional antennas are low gain which in turn constrains the receive power and hence the data rate of the system. Were highly directive (i.e., high gain) antennas to be used, then active attitude control and pointing systems would have to be used to ensure alignment between the satellite antenna and the ground station antenna between which is relative motion for LEO orbits. Murtaza (2011) outlined an Attitude and Orbit Determination and Control Subsystem (AODCS) design requirements. Preindl et al. (2009a), mention another function for this subsystem which is attenuation control so as to maximize the received signal at the ground station and to keep it constant.

Due to the small size and hence limited surface area of CubeSats, the average power that can be obtained via solar array panels that typically cover the body of the satellite, is very low (Palo, 2015; Addaim et al., 2007). The primary power comes from the solar panels, and the secondary power from battery packs (Gao et al., 2009). Selva and Krejci (2012) concur that a conservative estimate of available power in CubeSats is on the order of 1W for a 1U. When estimating the power to be generated by the solar panels, the following parameters should be considered: the duration of the daylight exposure to the satellite; the solar cell efficiency and power generated per unit area; the inherent degradation of the solar panel and the degradation per year; the worst-case sun incident angle; and the total area available for the solar panel (Murtaza, 2011; Lee et al., 2013).

When determining the power generated by the batteries, the parameters for consideration include the duration of each eclipse ; the number of eclipses, and the Depth of Discharge (DOD) of the battery (Murtaza, 2011). The mass of the solar array as well as the mass of the battery must be taken into account in the mass budget which also deducts from the power budget. Ravanbakhsh and Franchini (2013) presented solar array sizing and battery sizing procedures. They highlighted the mass and power budget equations of the System Engineering Design Tool (SEDT) created by Chang et al. (2007) which were trendlines relating mass of subsystems with the total mass of the system and power allocated to subsystems versus the total power available to the system based on data obtained from 200 small satellites launched between 1990 and 2004. However, the lower limit is 10 kg satellite mass which is above the range for CubeSats.

Radiation and thermal control is another consideration in satellite design. Addaim et al. (2007) mention two categories of radiation effects: total radiation dose and Single-Event Effects (SEE). The total radiation dose a nanonsatellite can experience is 25 rads, however CMOS technology can survive approximately 5k rads. The SEE are more destructive and can manifest as Single Event Upset (SEU), Single Event Transient (SET) or Single Event Latch-up (SEL). The first two do not cause physical damage but the latter can. These can result in four bit-errors per day and less than two latch-up per year. To limit radiation there should be suitable shielding of the electrical components. To limit the SET effect, lower clock speeds are recommended. Thermal control, according to Murtaza (2011), ensures that the satellite systems are kept within the stipulated temperature bounds (typically 0 to 30 degrees Celsius) regardless of the thermal environment. Thermal control can be active or passive and cost, power, weight and reliability influence the choice.

The structural design of the CubeSat must comply with the CubeSat design specification as stated by Mehrparvar et al. (2014), which has mass and volume restrictions and specifies electro-mechanical interfaces such as the deployment detection switch and the remove-before-flight switch (Schaffner 2002). And, can be made of 705 Aluminium (Waydo et al 2002).

3. Conclusion and Future Work

This paper focused on design considerations of the communication subsystem of the CubeSat system for the transfer of ADCP data via a satellite link. We did not treat with the underwater link between the ADCP device and the landing/pier. Options for this part of the communication link have been considered by Long (2014) using autonomous vehicle networks.

To summarize the design process: we determined the bandwidth requirements of the ADCP; designed the LEO constellation configurations for different orbital altitudes; determined, with the aid of AGI's STK simulation tool, the worst-case bit-rate that can be accommodated during the visible period; exploreddifferent frequency bands for transmission(with the UHF/VHF and the S-band being selected as likely candidates); performed antenna design; selected transceivers for the ground station and CubeSat; and calculated link budgets for the different altitudes.

Acknowledgments:

The authors would like to thank Dr. Cathy-Ann Radix of The University of the West Indies, for assisting us with the calculation of the ADCP bandwidth requirements.

References:

Addaim, A., Kherras, A. and Zantou, B. (2007), "Design of store and forward data collection low-cost nanosatellite", *Proceedings of the IEEE Aerospace Conference*, Big Sky, Montana, USA, March, pp.1-10.

AGI (2019), "AGI Systems Tool Kit (STK)", [online], Available at: https://www.agi.com/products/satellite-design-and-operations [Accessed 05 Apr. 2019].

Akagi, J., Tamashiro, T., Iwami, R., Cardenas, J., Akagi, J. and Shiroma, W. (2008), "Cubesat-based disaster detection and monitoring systems", *Proceedings of the 6th Responsive Space Conference*, Los Angeles, CA.,

http://citeseerx.ist.psu.edu/viewdoc/download?doi=10.1.1.559.4014&rep=rep1&type=pdf

Balanis, C. (2005), Antenna theory, Analysis and Design, 3rd edition, John Wiley & Sons Inc.

Blas, A.C. (2009), *Kumu A'O Cubesat Telecommunication Subsystem Antenna Design, Testing, and Mounting*, Hawaii Space Grant Consortium, Undergraduate Fellowship Reports, Report Number 09-18.

Chang, Y.-K., Hwang, K.-L., and Kang, S.-J. (2007), "SEDT (System Engineering Design Tool) development and its application to small satellite conceptual design", *Acta Astronautica*, Vol.61, No.7, pp.676-690.

Chen-Tung, A.C. and Nihoul, J. C. J., (2009)(ed), *Encyclopedia of Life Support Systems: Oceanography*, Vol. III, EOLSS Publications.

Costantine, J., Tawk, Y., Maqueda, I., Sakovsky, M., Olson, G., Pellegrino, S. and Christodoulou, C.G. (2016), "UHF deployable helical antennas for CubeSats", *IEEE Transactions on Antennas and Propagation*, Vol.64, No.9, pp.3752-3759.

Fossa, C.E., Raines, R.A., Gunsch, G.H. and Temple, M.A. (1998), "An overview of the IRIDIUM (R) Low Earth Orbit (LEO) Satellite System", *Proceedings of the IEEE 1998 National Aerospace and Electronics Conference (NAECON 1998). Celebrating 50 Years (Cat. No.98CH36185)*, 17 July 1998, pp.152-159.

Gagliardi, R.M. (1984), *Satellite Communications*, Van Nostrand Reinhold, New York

Gao, S., Clark, K., Unwin, M., Zackrisson, J., Shiroma, W.A., Akagi, J. M., Maynard, K., Garner, P., Boccia, L., Amendola, G., Massa, G., Underwood, C., Brenchley, M., Pointer, M. and Sweeting, M.N. (2009), "Antennas for modern small satellites", *IEEE Antennas and Propagation Magazine*, Vol.51, No.4, pp.40-56.

He, R., Ai, B., Wang, G., Guan, K., Zhong, Z., Molisch, A.F., Briso-Rodriguez, C. and Oestges, C.P. (2016), "High-speed railway communications: From GSM-R to LTE-R", *IEEE Vehicular Technology Magazine*, Vol.11, No.3, pp.49-58.

Ichikawa, D. (2006), *Cubesat-To-Ground Communication and Mobile Modular Ground- Station Development*, HSGC Report Number 07-15:34.

ITU (2005), "Recommendation ITU-R P.838-3: Specific attenuation model for rain for use in prediction methods", International Telecommunication Union, Available from http://www.ecs.umass.edu/ece597ap/References/R-REC-P.838-3-200503-I!!PDF-E.pdf

Julio, Y.E.R. (2016), "Design Ubiquitous Architecture for Telemedicine based on mhealth Arduino 4G LTE", Proceedings of the 18th IEEE International Conference on e-Health Networking, Applications and Services (Healthcom), Munich, Germany,14-16 September, pp.1-6.

Jun-lin, W. and Chun-sheng, L. (2011), "Development and application of INMARSAT satellite communication system", *Proceedings of the First International Conference on Instrumentation, Measurement, Computer, Communication and Control*, Beijing, China,21-23 October, pp.619-621.

Khurshid, K., Mahmood, R. and ul Islam, Q. (2013), "A survey of camera modules for CubeSats: Design of imaging payload of ICUBE-1", *Proceedings of the 6th International Conference on Recent Advances in Space Technologies (RAST)*, Istanbul, Turkey, 12-14 June, pp.875-879.

Kiremitci, H. (2013), *Satellite Constellation Optimization for Turkish Armed Forces*, MSc Report, Naval Postgraduate School , California, USA.

Kong, L., Jin, J. and Cheng, J. (2005), "Introducing GPRS technology into remote monitoring system for prefabricated substations in China", *Proceedings of the 2nd Asia Pacific Conference on Mobile Technology, Applications and Systems*, Guangzhou, China,15-17 November, pp.6.

Leao, T.F.C., Mooney-Chopin, V., Trueman, C.W. and Gleason, S. (2013), "Design and implementation of a diplexer and a dual-band VHF/UHF antenna for nanosatellites", *IEEE Antennas and Wireless Propagation Letters*, Vol.12, pp.1098-1101.

Lee, J., Kim, E. and Shin, K.G. (2013), "Design and management of satellite power systems", *Proceedings of the IEEE 34th Real-Time Systems Symposium*, Vancouver, BC, Canada ,3-6 December, pp.97-106.

Long, F. (2014), *Satellite Network Robust QoS-aware Routing*, Springer.

Mehrparvar, A., Pignatelli, D., Carnahan, J., Munakata, R., Lan, W., Toorian, A., Hutputanasin, A. and LeeS. (2014), *CubeSat Design Specification*, California Polytechnic State University, Cal Poly SLO.

Muri, P., Challa, O. and McNair, J. (2010), "Enhancing small satellite communication through effective antenna system design", *Proceedings of the Milcom 2010 Military Communications Conference*, San Jose, California, USA ,31 October - 3 November, pp.347-352.

Murtaza, H. (2011), "Designing a small satellite in LEO for remote sensing application", *Journal of Space Technology*, Vol.1, No.1, pp. 6.

Palo, S.E. (2015), "High rate communications systems for CubeSats", *Proceedings of the IEEE MTT-S International Microwave Symposium*, Phoenix, AZ, USA, 17-22 May, pp.1-4.

Pedersen, L., Smith, T., Lee, S.Y. and Cabrol, N. (2015), "Planetary LakeLander: A robotic sentinel to monitor remote lakes", *Journal of Field Robotics*,, Vol.32, No.6, pp.860-879.

Pittella, E., Pisa, S. and Nascetti, A. (2013), "Design of an antenna system for CubeSat satellites", *Proceedings of the 2nd IAA Conference on University Satellites Missions and CubeSat Winter Workshop*, Roma, Italy, 3 -9 February 2013, pp.1-6

Popescu, O., Harris, J.S. and Popescu, D.C. (2016), "Designing the communication sub-system for nanosatellite CubeSat missions: Operational and implementation perspectives", *Proceedings of the Southeast Conference*, Norfolk, VA, USA , 30 March - 3 April, pp.1-5.

Preindl, B., Mehnen, L., Rattay, F. and Nielsen, J.D. (2009a), "Design of a small satellite for performing measurements in a ground station network", *Proceedings of the International Workshop on Satellite and Space Communications*, Siena, Italy ,9-11 September, pp.186-190.

Preindl, B., Mehnen, L., Rattay, F., Nielsen, J.D., Krinninger, S. and Sørensenz, K.K. (2009b), "A global satellite link sensor network", *Proceedings of the IEEE Sensors Conference*, Christchurch, New Zealand,, 25-28 October, pp.1400-1405.

Ratasuk, R., Iraji, S., Hugl, K., Wang, G. and Ghosh, A. (2013), "Performance of low-cost LTE devices for advanced metering infrastructure", *Proceedings of the IEEE 77th Vehicular Technology Conference (VTC Spring)*, Dresden, Germany , 2-5 June, pp.1-5.

Ravanbakhsh, A. and Franchini, S. (2013), "System engineering approach to initial design of LEO remote sensing missions", *Proceedings of the 6th International Conference on Recent Advances in Space Technologies (RAST)*, Istanbul, Turkey , 12-14 June, pp.659-664.

Rodríguez-Osorio, R.M. and Ramírez, E.F. (2012), "A hands-on education project: Antenna design for inter-CubeSat communications [Education Column]", *IEEE Antennas and Propagation Magazine*, Vol.54, No.5, pp.211-224.

Schaffner, J. A. (2002), "The electronic system design, analysis, integration, and construction of the Cal Poly State University CP1 CubeSat", *Proceedings of the 16th AIAA/USU Conference on Small Satellites*, Utah State University, Utah, 12 – 15 August, pp.1-12.

Selva, D. and Krejci, D. (2012), "A survey and assessment of the capabilities of Cubesats for earth observation", *Acta Astronautica*, Vol.74, pp.50-68.

Shiroma, W. A., Akagi, J.T., Ohta, A. T., Akagi, J. M. and Wolfe, B.L. (2012), "Small satellites for rapid-response communication and situational assessment", *Proceedings of the IEEE International Conference on Wireless Information Technology and Systems (ICWITS)*, Maui, Hawaii, USA, 11-16 November, pp.1-4.

Stapko, T. (2010), "DesignLines Internet-of-Things Design How-To: Cryptography for embedded systems - Part 1: Security level categories and hashing", [online], Available at: https://www.eetimes.com/document.asp?doc id=1278110 [Accessed 01 Oct. 2017].

Teledyne RD Instruments (2013), *Workhorse Sentinel, Monitor and Mariner Operation Manual*, (ISBN 957-6150-00), Teledyne RD Instruments, Poway, CA 92064, USA

Teledyne RD Instruments (2019), "Teledyne Acoustic Modems", [online], Available at: http://www.teledynemarine.com/acoustic-modems [Accessed 5 Apr. 2019].

Waydo, S., Henry, D. and Campbell, M. (2002), "CubeSat design for LEO-based earth science missions", *Proceedings of the IEEE Aerospace Conference*, Big Sky, Montana, USA,, 9-16 March, pp.1-1.

Weinert, A.J., Breimyer, P., Devore, S. M., Miller, J. M., Brulo, G. S., Teal, R.S., Zhang, D., Kummer, A.T. and Bilén, S. G. (2012), "Providing communication capabilities during disaster response: Airborne Remote Communication (ARC) platform", *Proceedings of the IEEE Conference on Technologies for Homeland Security (HST)*, Waltham, MA, USA ,13-15 November, pp.395-400.

Wilson, M.J. (2007), *The ARRL Operating Manual for Radio Amateurs*, The American Radio Relay League, Inc., Newington, CT 06111, USA

Zhao, L., Huo, C. and Yang, H. (2012a), "The design of remote video monitoring system based on S3C2416 and GPRS", *Proceedings of the International Conference on System Science and Engineering (ICSSE)*, Dalian, Liaoning, China, 30 June - 2 July, pp.385-388.

Zhao, X., Zhang, Z. and Meng, W. (2012b), "GPRS based remote data acquisition and forecasting system for long-distance natural Gas pipeline monitoring", *Proceedings of the International Conference on Computational Problem-Solving (ICCP)*, Leshan, China, 19-21 October, pp.504-507.

Authors' Biographical Notes:

Richelle V. Adams *received the B.Sc. degree in Electrical and Computer Engineering in 1998 and the M.Sc. degree in Communication Systems in 2001 from The University of the West Indies, St. Augustine Campus, Trinidad and Tobago. In 2007, she received the Ph.D. degree in Electrical and Computer Engineering from the Georgia Institute of Technology, Atlanta, USA. In 2011, she was a Visiting Fulbright Scholar at the Institute for Crisis, Disaster and Risk Management, George Washington University, Washington, D.C., USA. She is Lecturer in the Department of Electrical and Computer Engineering, The University of the West Indies.*

Deborah Villarroel-Lamb *is Lecturer in the Department of Civil and Environmental Engineering at The University of the West Indies, St. Augustine. She specializes in coastal engineering, which includes ocean hydrodynamics, coastal morphology and coastal engineering solutions.*

Fasil Muddeen *is Lecturer in the Department of Electrical and Computer Engineering at The University of the West Indies. His areas of research include digital signal processing, the acoustics of the Caribbean steelpan, electronics and instrumentation. Dr. Muddeen is a registered engineer with the Board of Engineering of Trinidad and Tobago and is a past Chairman of the IEEE Trinidad and Tobago Section.*

■